Check for updates

Carbon–carbon bond activation by Mg, Al, and Zn complexes

Joseph M. Parr and Mark R. Crimmin (ID) *

Examples of carbon–carbon bond activation reactions at Mg, Al, and Zn are described in this review. Several distinct mechanisms for C–C bond activation at these metals have been proposed, with the key C–C bond activation step occurring by (i) α-alkyl elimination, (ii) β-alkyl elimination, (iii) oxidative addition, or (iv) an electrocyclic reaction. Many of the known pathways involve an overall 2-electron redox process. Despite this, the direct oxidative addition of C–C bonds to these metals is relatively rare, instead most reactions occur through initial installation of the metal on a hydrocarbon scaffold (*e.g.* by a cycloaddition reaction or hydrometallation) followed by an α-alkyl or β-alkyl elimination step. Emerging applications of Mg, Al, and Zn complexes as catalysts for the functionalisation of C–C bonds are also discussed.

1. Introduction

Carbon–carbon (C–C) bonds are ubiquitous, making up the hydrocarbon skeleton of most organic molecules. Reactions that break strong C–C bonds are therefore of broad importance. For example, selective activation of C–C bonds affords a powerful method to alter the hydrocarbon scaffold of molecules.[1,2] This opens the door for novel synthetic disconnections and routes to complex organic molecules of relevance to medicinal and materials chemistry. Reactions that break C–C bonds also underpin our global energy sector. Globally essential fuels (coal, crude oil, and biomass) are comprised of C–C bonds. Catalytic cracking of C–C bonds in hydrocarbon feedstocks, such as crude oil, converts high molecular weight alkanes to more valuable alkenes and medium-length hydrocarbons (*e.g.* C_7 to C_9 alkanes).[3–5]

Reactions that break C–C bonds are challenging to achieve.[6] C–C bonds are strong and non-polar. To give two examples: (i) ethane, the simplest linear alkane, has a homolytic bond dissociation energy[7] of 90.1 ± 0.1 kcal mol^{-1}, (ii) benzene has a calculated homolytic bond dissociation energy[8] of 147.0 kcal mol^{-1}. The increased thermodynamic stability of C–C bonds in aromatic rings is unsurprising given their π-character and electron delocalisation across the ring. C–C bonds are also sterically protected. They are often buried within the molecular framework and the orbitals involved in bonding are kinetically inaccessible. As such chemoselectivity becomes a key issue, with surrounding C–H bonds often the first sites to react with reagents and catalysts that would otherwise be capable of breaking C–C bonds.[9]

Department of Chemistry, Molecular Science Research Hub, Imperial College London, 82 Wood Lane, White City, London, W12 0BZ, UK. E-mail: m.crimmin@imperial.ac.uk

Here we define C–C bond activation as a process in which the C–C bond of the σ-framework breaks at a metal centre (M), creating at least one new M–C bond. While C–C bond functionalisation is defined as a process that breaks a C–C bond and transforms into two new C–X bonds (X = H, heteroatom). The activation of C–C bonds has been achieved on the surface of heterogeneous catalysts,[10] within the active sites of enzymes,[11,12] and under homogeneous conditions using metal complexes.[13,14] The systems which are best understood are arguably those that contained well-defined transition metal sites (Co–Ir, Ni–Pt),[15] where partially occupied valence d-orbitals facilitate C–C bond breaking.[16–18] Often model substrates that contain weakened C–C bonds and/or extensive ring strain are studied.[19] For example, hydrocarbons with smaller ring sizes are routinely investigated as the C–C bond strength decreases across the series cyclohexane > cyclopentane > cyclobutane > cyclopropane.[20–22] Reactivity tends to follow established mechanisms (Scheme 1).

• (A) β-Alkyl elimination, wherein a metal bound alkyl ligand is fragmented into the corresponding metal alkyl and alkene units.[23,24]

• (B) Oxidative addition, wherein the C–C bond is cleaved by addition to a low oxidation state metal complex, increasing the metal oxidation state by two and creating two new M–C bonds.[17]

• (C) Cycloaddition between a hydrocarbon and metal reagent, creating a strained metallocycle which can then undergo C–C bond activation (*e.g.* through α-elimination or an electrocyclic reaction).[25,26]

Though important progress is being made toward transition metal mediated C–C bond activation, there is an increasing drive away from late transition metal-based systems. Late transition metals are commonly expensive and toxic, with further issues regarding the sustainability and ethics of the mining practices used to obtain the requisite minerals for

Mechanism A: β-alkyl elimination
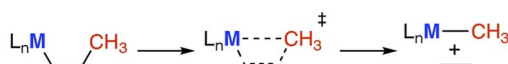
Mechanism B: Oxidative addition

Mechanism C: Initiated by a cycloaddition

Scheme 1 Carbon−carbon bond activation mechanisms, via (A) β-alkyl elimination or migration; (B) oxidative addition; (C) cycloaddition reaction and subsequent rearrangement.

Scheme 2 Early examples of β-alkyl elimination at main group metals. The reversible release of iso-butene gas by thermolysis of tris(neo-pentyl)aluminium **1** (top); elimination of iso-butene gas during mass-spectrometer fragmentation of tris(neo-pentyl)stannyl cation **2** (bottom), R = CH_2CMe_3.

refining.[27,28] Main-group metals (e.g. Mg, Al) along with the post-transition metal Zn are promising alternatives to their transition metal counterparts for applications in synthesis and catalysis. These elements are commonly earth-abundant, inexpensive, and more widely distributed in the Earth's crust compared to the late transition metals.[29] They are non-toxic and accordingly safer to handle. For some (e.g. Al) there are even established networks and processes for recycling, auguring well for a future circular economy.

In this review, we summarise the current examples of C−C bond activation with Mg, Al, and Zn complexes. The scope of the review is limited to these emerging systems with a specific focus on mechanism and understanding. To the best of our knowledge there are no well-defined examples of C−C bond activation with heavier main group (Ca−Ba, Ga−Tl, Pb), or post-transition (Cd−Hg) metals. A limited number of examples of metal free C−C bond activation have been reported for systems using frustrated Lewis pairs,[30] boron-,[31,32] silicon-,[33–35] phosphorous,[36,37] and organic-compounds.[38] These examples with non-metals or semi-metals are not the focus of this review and are covered elsewhere.[39] The discussion is split into three distinct approaches, namely β-alkyl migration, oxidative addition, and those initiated by cycloaddition reactions. Through discussion of mechanism, we aim to highlight the divergent chemistry shown by these complexes compared to their transition metal counterparts and touch on the potential implications in synthesis.

2. Carbon−carbon bond activation

2.1 β-Alkyl elimination at Mg and Zn metal centres

One of the earliest reports of C−C σ-bond activation by any metal appears to proceed through a β-alkyl migration mechanism at an aluminium centre. In 1960, Pfohl reported the thermolysis of tris(neo-pentyl)aluminium [Al{CH$_2$C(Me)$_3$}$_3$] **1** at high temperature (200 °C).[40] The reversible stoichiometric formation of iso-butene gas and trimethylaluminium was observed via sp^3 C−C σ-bond activation, presumed to occur through a β-methyl migration reaction (Scheme 2). The release
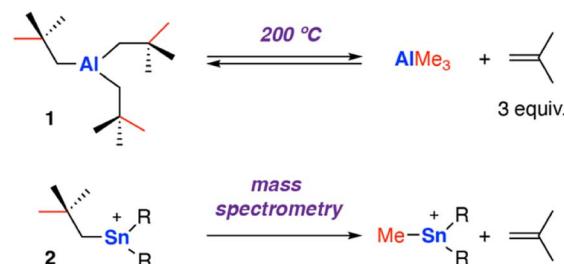
of three equivalents of iso-butene gas provides an entropic driving force for the forward reaction.

In 1999, Dakternieks and co-workers reported a related reaction at a Sn complex, observed during fragmentation in a mass spectrometer.[41] Application of a high cone voltage (>60 V) to a acetonitrile solution of the tris(neo-pentyl)stannyl cation [Sn{CH$_2$C(Me)$_3$}$_3$]$^+$ **2** showed formation of methyl tin cations and release of isobutene gas. Reaction of the deuterium labelled analog [Sn{CD$_2$C(Me)$_3$}$_3$]$^+$ showed the formation of isobutene gas with the alkene protons D-labelled, consistent with a β-alkyl elimination process. An alternate pathway involving homolysis of the Sn−C bond to form a neo-pentyl radical that fragments to iso-butene and a methyl radical that can recombine with Sn, was not ruled out and cannot be discounted under fragmentation conditions in the mass spectrometer.

In 2020, we reported C−C σ-bond cleavage of strained alkylidene cyclopropanes using magnesium reagents.[42] Reaction of the β-diketiminate stabilised magnesium(I) dimer [Mg{CH{C(CH$_3$)NMes}$_2$}]$_2$ (Mes = 2,4,6-trimethylphenyl)[43–46] **3** with alkylidene cyclopropanes **4a–b** and subsequent addition of dimethylaminopyridine (DMAP) led to the corresponding ring-opened products **5a–b·DMAP** (Scheme 3). DMAP was used to trap and help crystallise the products and is not thought to participate in the mechanism of C−C σ-bond activation. DFT calculations support a stepwise mechanism starting with 1,2-addition of the Mg–Mg σ-bond to the alkene.[47] This step places one of the Mg sites in a suitable position to facilitate β-alkyl migration. β-Alkyl migration from the 1,2-dimagnesio-ethane intermediate is then a relatively facile process ($\Delta G^{\ddagger}_{298\ K}$ = 12.7 kcal mol^{-1}), yielding the observed products.

This work was extended to include reaction of the related magnesium(II) hydride complex **6** [Mg(μ-H){CH{C(CH$_3$)NDipp}$_2$}]$_2$ (Dipp = 2,6-diisopropylphenyl) with the same set of substrates (Scheme 3, bottom).[48,49] Stoichiometric reaction of **6** with methylidene cyclopropane (**7a**) and methylidene cyclobutane (**7b**) yielded the ring-opened alkyl magnesium complexes **9a** and **9b** in good yields. Though no intermediates were observed spectroscopically, DFT calculations and related literature[23,50,51] supported a hydromagnesiated intermediate **8a–b** as a prerequisite to β-alkyl elimination and thus C−C σ-bond activation. Additional evidence for the hydromagnesiated
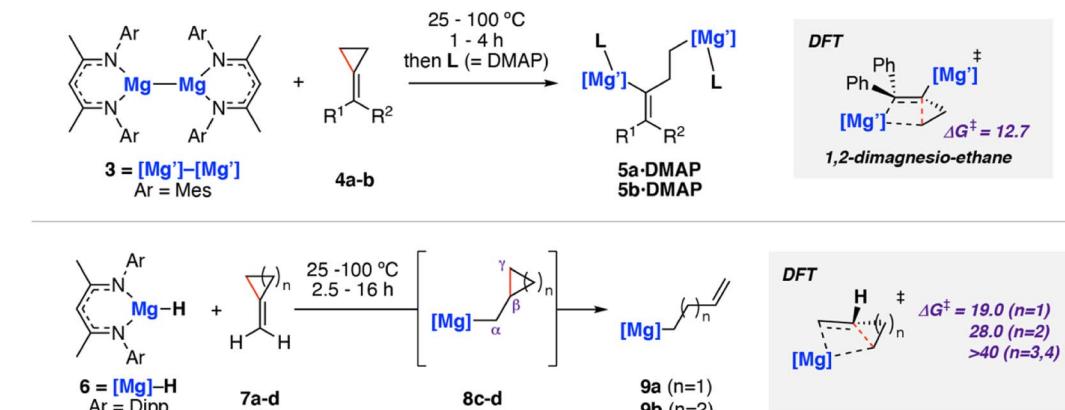
Scheme 3 Reaction of magnesium(I) complex **3** with methylidene cycloalkanes **4a–b** (top). Reaction of magnesium(II) hydride complex **6** with **7a–d** (bottom). Mes = 2,4,6-trimethylphenyl; Dipp = 2,6-diisopropylphenyl. Energies for $\Delta G^{\ddagger}_{298\ K}$ in kcal mol^{-1}. **4a** (R^1 = R^2 = Ph), **4b** (R^1 = Ph, R^2 = H), **7a–d** ($n = 1–4$).

intermediates was gathered through reaction of unstrained methylidene cyclopentane (**7c**) and methylidene cyclohexane (**7d**) with **6**, which formed the hydromagnesiated products **8c–d** in high yields.[52] Calculated activation barriers for σ-bond C–C bond cleavage for five and six-membered rings were unfeasible under the reaction conditions ($\Delta G^{\ddagger}_{298\ K} > 40$ kcal mol^{-1}), indicating that the release of ring strain in the three- and four-membered systems is an important driving force for the reaction.

The analogous zinc hydride complex [ZnH{CH{C(CH$_3$) NDipp}$_2$}][53] **10** was shown to react with methylidene cyclopropane **7a** in a similar fashion.[49] The resulting zinc alkenyl complex **12** was isolated in high yield and characterised. In the case of zinc, the proposed hydrozincated intermediate **11** was observed spectroscopically (Scheme 4). Diagnostic resonances in the ^{1}H NMR spectra at $\delta = -0.39$ to -0.36 and $\delta = 0.15$ to 0.20 ppm were assigned to **11** through application of HSQC and TOCSY NMR methods. DFT calculations support a stepwise hydrometallation and subsequent β-alkyl elimination pathway. The activation barrier for C–C cleavage was calculated as $\Delta G^{\ddagger}_{298\ K} = 35.2$ kcal mol^{-1}, in line with the high temperature conditions required for the reaction.

Scheme 4 Stoichiometric reaction of zinc hydride complex **10** with methylidene cyclopropane **7a**, forming the ring-opened zinc complex **12** via C–C σ-bond activation at Zn. Ar = 2,6-diisopropylphenyl. Energies for $\Delta G^{\ddagger}_{298\ K}$ in kcal mol^{-1}.

Activation strain analysis[54,55] was used to explain the differences in reactivity between the analogous zinc and magnesium hydride complexes. Namely, that magnesium was observed to ring open cyclobutane rings, whereas zinc was not. The more electropositive metal (Mg) was shown to be better able to stabilize the hydrocarbon fragment at the C–C activation transition state, lowering the kinetic barrier relative to Zn.[49] **6** and **10** have an identical ligand coordination, as such it can be concluded that chemoselectivity in these reactions can be controlled through choice of the metal.

Reaction of the magnesium alkenyl complex **9a** with an excess of phenyl silane (PhSiH$_3$) led to formation of the linear and cyclic silane compounds **13–14** and reformation of magnesium hydride **6**. A catalytic protocol for the hydrosilylation of strained σ-C–C bonds was developed from these findings.[42,49,56,57] Reaction of **4a–b** and **7a–b** with excess phenyl silane and 10 mol% of **6** showed high conversion to the respective cyclic silanes **14–15**. In the case of **4b**, catalytic hydrosilylation yields a mixture of E and Z stereoisomers of the products **16–17**, with a ratio of $E : Z$ of 1 : 1.1. Scheme 5 shows the proposed catalytic cycle, each step of which is supported by experimental and computational data. The stepwise process follows: (i) hydromagnesiation of the alkene through a 1,2-insertion reaction of the magnesium hydride to the alkene (ii) β-alkyl migration; (iii) σ-bond metathesis to regenerate magnesium hydride catalyst **6** and the linear silane. The thermodynamic products **14–15** are likely formed from an intramolecular hydrosilylation also catalysed by the magnesium complex **6**. The related zinc complex **10** was unable to catalyse the hydrosilylation of the σ-C–C bond of **7a**, again highlighting the divergent reactivity of main-group and post-transition metals in these systems.[49]

The most likely origin of these differences is the σ-bond metathesis step of the proposed catalytic cycle which while operating with Mg, is likely too slow to facilitate turnover with Zn.
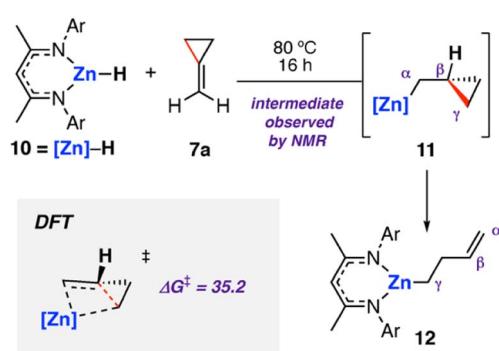
2.2 Oxidative addition at aluminium centres

Oxidative addition, and its microscopic reverse, reductive elimination, are some of the most fundamental
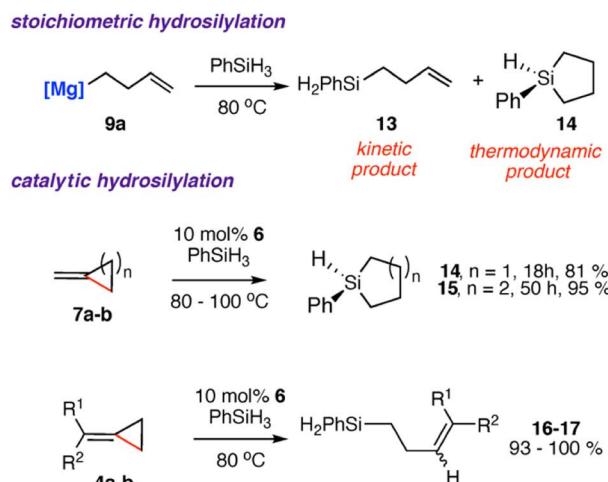
Scheme 5 Stoichiometric and catalytic hydrosilylation of alkylidene cycloalkanes **4a–b**, **7a–b** using a molecular magnesium hydride reagent **6** (left). Proposed catalytic cycle (right). [Mg] = [Mg{CH(C(CH$_3$)NDipp)$_2$}], Dipp = 2,6-diisopropylphenyl. **16**, R^1 = R^2 = Ph; **17**, R^1 = Ph, R^2 = H.

transformations in organometallic chemistry. Biphenylene has been the subject of detailed study in transition-metal mediated C–C σ-bond activation *via* oxidative addition. Recent examples have extended study of the substrate to low-valent aluminium complexes. Biphenylene comprises two benzene rings fused by a central C$_4$ ring. The central C–C σ-bond of the four-membered has a low bond dissociation energy of 65.4 kcal mol^{-1}.[58,59] Both the anti-aromatic character and strain of the four-membered ring contribute to the weakening of this C–C σ-bond. In contrast, the C–C bond strength within the six-membered ring system has been estimated as 114.4 kcal mol^{-1}. Addition of transition metals to biphenylene results exclusively in σ-C–C bond activation *via* oxidative addition at the central C$_4$ ring (M = Fe, Co, Ni, Ru, Rh, Pd, Os, Ir, Pt, Au).[60–65] Very recently, selective cleavage of the C–C bonds in biphenylene during potassium reduction of rare-earth metal complexes (Sc, Lu) was reported.[59]

In 2020, Kinjo and co-workers reported an aluminyl anion stabilised by a cyclic (alkyl)(amino) ligand, prepared by potassium graphite reduction of the corresponding aluminium dimer in the presence of 12-crown-4.[66] The resulting aluminyl anion **18** [Al{NAd(CH)$_2$C(SiMe$_3$)$_2$}][K(12-C-4)$_2$] was shown to react with biphenylene at room temperature over the course of four hours (Ad = 1-adamantyl, 12-C-4 = 12-crown-4). Oxidative addition of the weakest C–C σ-bond in biphenylene (in the strained four membered ring) was observed (Scheme 6). The metallocyclic anionic complex **19** was isolated in moderate yield (33%) and crystallographically characterised. The overall reaction can be categorised as a two-electron oxidative addition reaction at Al, from Al(I) to Al(III). Oxidative addition of the central four membered ring of biphenylene is well known for most transition metals, with this work extending the concept to main-group metal complexes for the first time. DFT calculations, performed by Zhu and co-workers, suggest C–C σ-bond activation of benzene by **18** could become both kinetically and thermodynamically favourable through addition of electron withdrawing groups onto benzene.[67] In practice though,

inclusion of additional functionality raises the issue of chemoselectivity; most of these functional groups would contain C–X (X = heteroatom) bonds that are likely to react in preference to the C–C bond.

2.3 C–C bond activation initiated by cycloadditions

In 2020, we reported the reaction of a β-diketiminate stabilised aluminium(I) nucleophile[71] **20** with a series of unsaturated cyclopropanes **4a–d**, **7a** (Scheme 7). Take 1,1'-(cyclopropylidenemethylene)dibenzene (**4a**, R^1 = R^2 = Ph) as a representative example. Reaction of **20** with **4a** initially formed an Al(III) metallocyclopentane complex **21** *via* a (4 + 1) cycloaddition. DFT calculations show a low energy barrier ($\Delta G^{\ddagger}_{298 \text{ K}}$ = 14.1 kcal mol^{-1}) for the exergonic formation of **21** from **20** and **4a** ($\Delta G^{\circ}_{298 \text{ K}}$ = –14.2 kcal mol^{-1}). Heating crude or isolated samples of **21** resulted in C–C σ-bond activation of the cyclopropane ring and formation of metallocyclobutane complex **22**. The reaction proceeded rapidly at 100 °C (<15 min) or slowly
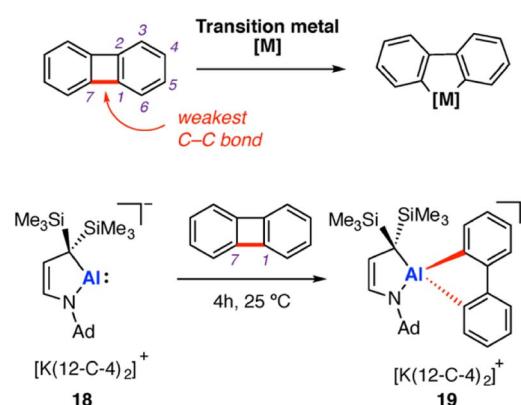
Scheme 6 Labelled biphenylene substrate and reported reactivity with transition metals (top); reaction of **18** with biphenylene, resulting in C–C σ-bond scission *via* oxidative addition of the central C^1–C^7 σ-bond (bottom). Ad = 1-adamantyl.
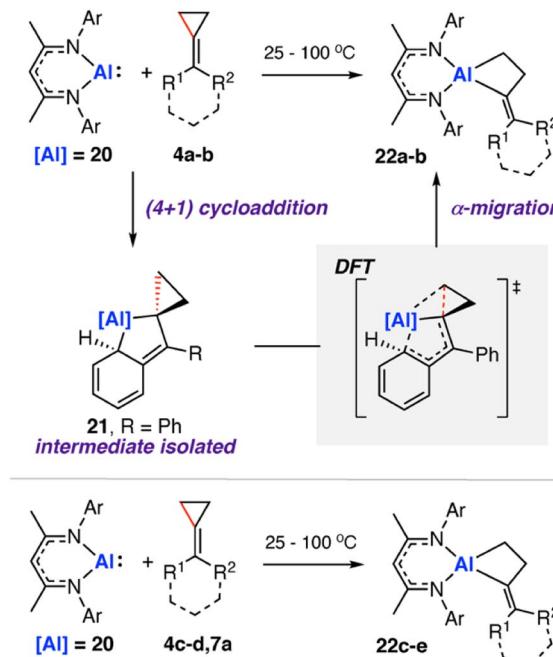
Scheme 7 Reaction of aluminium(I) nucleophile **20** with a series of methylidene cycloalkanes **4a**, $R^1 = R^2 = Ph$; **4b** $R^1 = Ph$, $R^2 = H$; **4c** $R^1 = R^2 = -(CH_2)_5-$; **4d** $R^1 = Cy$, $R^2 = H$; **7a** $R^1 = R^2 = H$; **22a** $R^1 = R^2 = Ph$; **22b** $R^1 = Ph$, $R^2 = H$; **22c** $R^1 = R^2 = -(CH_2)_5-$; **22d** $R^1 = Cy$, $R^2 = H$; **22e** $R^1 = R^2 = H$).

Scheme 8 Reaction of aluminum(I) nucleophile **20** with biphenylene, giving a mixture of products formed *via* C–C σ-bond cleavage. Ar = 2,6-diisopropylphenyl; NMR yield shown for product mixture.

(over a few days) at ambient temperature. Relief of ring strain provides a thermodynamic driving force for the overall reaction. DFT calculations suggest an α-migration pathway connecting intermediate **21** with the C–C activated product **22** ($\Delta G^{\ddagger}_{298\ K} = 25.8$ kcal mol^{-1}). The scope was extended to four other alkylidene cyclopropanes, showing a related α-migration pathway for C–C σ-bond activation at the Al(I) centre. For methylidene cyclopropanes with alkyl substituents, **4c–d**, reaction with **20** is presumed to occur through an initial (2 + 1) cycloaddition intermediate, as the (4 + 1) cycloaddition becomes inaccessible. For comparison, the direct oxidative addition of a C–C σ-bond in **4a** by **20** was calculated to proceed *via* a considerably higher energy transition state ($\Delta G^{\ddagger}_{298\ K} = 35.3$ kcal mol^{-1}). The data suggests the key factor for C–C σ-bond scission is not dependent on a redox reaction at the aluminium centre, rather on the installation of the electropositive Al atom in the correct position on the hydrocarbon scaffold to facilitate the α-alkyl migration rearrangement.

In 2021, our group reported the reaction of **20** with biphenylene.[75] This was the first report of chemoselective C–C bond activation of biphenylene, and a rare example where the substrate bias is overcome by reagent control. Reaction of two equivalents of **20** with biphenylene and heating to 100 °C yielded a mixture of metallocyclic complexes **25** and **26** in which aluminium(III) centres are incorporated in five-membered rings (Scheme 8). **25** and **26** are derived from the cleavage of the C^2–C^3 and C^4–C^5 bonds in the C_6 ring of biphenylene, respectively. These complexes can be separated. Heating purified samples of
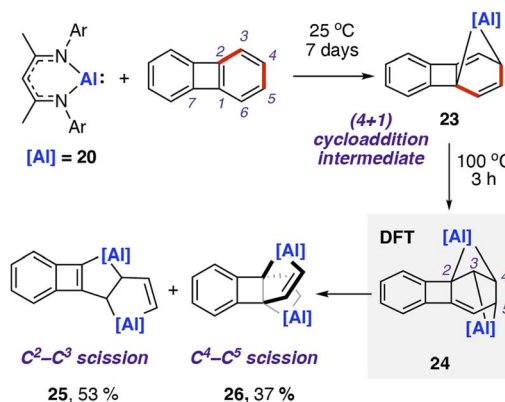
either product showed that they did not interconvert under the reaction conditions.

DFT calculations suggest an initial (4 + 1) cycloaddition reaction between **20** with biphenylene,[76] specifically a $[_\pi 4_s + _n 2_s]$ cycloaddition, yielding a highly strained and dearomatised hydrocarbon scaffold. The intermediate **23** can be isolated from the stoichiometric reaction of **20** with biphenylene at 25 °C for seven days. From **23**, DFT calculations suggest a pathway for addition of a second equivalent of **20** to the C_2–C_3 position and a subsequent concerted rearrangement to the more thermodynamically favourable isomer **24**. The isomerisation is likely driven by the interchange of the three- and five-membered rings within the first intermediate to two four-membered rings in the second intermediate, relieving ring strain in the system. From **24**, two similar energy pathways to products **25** and **26** are proposed, *via* either C–C bond cleavage and subsequent 1,3-sigmatropic shift, or a 1,3-sigmatropic shift followed by C–C bond cleavage. Both pathways are highly exergonic, consistent with the nonreversible formation of the products observed experimentally. A direct oxidative addition of the central C^1–C^7 σ-bond of biphenylene to **20** was calculated to occur by a high activation barrier ($\Delta G^{\ddagger}_{298\ K} = 42.0$ kcal mol^{-1}), likely to be inaccessible under the reaction conditions. Further calculations using activation strain analysis suggest that the inaccessible energy barriers for oxidative addition are likely a result of the strain required to achieve orbital overlap between the aluminium complex's lone pair and C^1–C^7 σ*-orbital in biphenylene.

In 2022, Liu and co-workers reported the synthesis of an N-heterocyclic carbene (NHC) stabilised aluminylene compound, featuring a bulky carbazolyl ligand **27**.[72–74] DFT calculations show a decreased HOMO–LUMO gap upon NHC coordination to **27** compared with the analogue without the additional coordinated ligand. **27** was shown to reversibly convert into the aluminocyclic complex **28** formed by an intramolecular insertion of Al into the flanking 3,5-di-*tert*-butylphenyl rings of **27**. DFT calculations support a reversible process ($\Delta G^{\circ}_{298\ K} = -4.5$ kcal mol^{-1}) *via* a concerted transition state ($\Delta G^{\ddagger}_{298\ K} = 25.6$ kcal mol^{-1}) to form the AlC$_6$ ring. Calculations

for the analogous pathway without NHC coordination showed a kinetically unfavourable activation barrier of $\Delta G^{\ddagger}_{298\ K} > 70$ kcal mol^{-1}.

Onward reaction of **27** with biphenylene at 100 °C resulted in the formation of the AlC$_6$ aluminocyclic complex **30** now derived from an intermolecular pathway (Scheme 9). Aromatic C–C bond scission occurred with the central (and weakest) C$_4$ unit remaining intact. This is the only report for the C–C bond cleavage of the C^5–C^6 bond in biphenylene for any metal. A (4 + 1) cycloaddition intermediate **29** was isolated from the reaction of **27** and biphenylene at 25 °C; a related (4 + 1) cycloaddition product was observed from reaction of **27** and naphthalene. DFT calculations suggest that C–C bond breaking can occur at intermediate **29**, albeit through a high energy transition state ($\Delta G^{\ddagger}_{298\ K} = 37.9$ kcal mol^{-1}). As this barrier is beyond what would be predicted for a process operating at 100 °C, alternative mechanisms for C–C bond, including bimetallic pathways, remain a possibility.

In 2019, Aldridge, Goicoechea, and co-workers reported the reversible room temperature C–C bond activation of benzene using a nucleophilic aluminium complex (Scheme 10).[68] Reaction of [K(2.2.2-crypt)][(NON)Al] (**31**, where NON = 4,5-bis(2,6-diiso-propyl-anilido)-2,7-di-*tert*-butyl-9,9-dimethylxanthene) with benzene at room temperature gave near quantitative formation of the corresponding aluminium(III) cycloheptatriene **33**. A cross-over experiment in which deuterium labelling C$_6$D$_6$ was added to **31** showed that the reaction is reversible, as evidenced by formation

d^6-**33** and C$_6$H$_6$ ($\Delta G^{\circ}_{(298\ K)} = -4.0$ kcal mol^{-1}). Addition of Me$_2$SnCl$_2$ to **33** generated the *Z,Z,Z*-isomer of the dimetallated heptatriene, Me$_2$ClSnCH=CH–CH=CH–CH=CHSnClMe$_2$ (**34**), derived from benzene. The aluminocycle **33** formed by C–C bond activation was shown to be a kinetic product that formed reversibly. When samples were heated to 80 °C non-reversible C–H activation of the benzene ring was observed. A subsequent computational investigation by Fernández and co-workers explored the competing C–C and C–H bond activation of benzene by **31** using a combination of activation strain and energy decomposition analyses.[69] Calculations support C–C bond activation as a kinetic pathway, as observed experimentally. The overall oxidative addition occurs through a stepwise mechanism, initiated by a (2 + 1)[70] cycloaddition reaction to form an aluminocyclopropane intermediate **32**. A 6π electrocyclic ring-opening of the aluminocyclopropane **32**, formally a Büchner ring expansion, cleaves the C–C bond to give **33** in an exergonic process ($\Delta G^{\ddagger}_{298\ K} = 23.2$ kcal mol^{-1}; $\Delta G^{\circ}_{298\ K} = -4.0$ kcal mol^{-1}). Reaction of **31** with naphthalene gave the C–H activation product only.

In 2021, Kinjo and co-workers reported a dianionic dialane complex **35** featuring an Al$_2$O three-membered ring supported by two K$^+$ ions. **35** was formed by the reduction of the corresponding dialane and subsequent treatment with triethylphosphine oxide.[77] Onward reaction of **35** with a series of small molecules, including biphenylene, was investigated (Scheme 11). Stoichiometric reaction of **35** with biphenylene at room temperature yielded a colourless precipitate (**37**) isolable
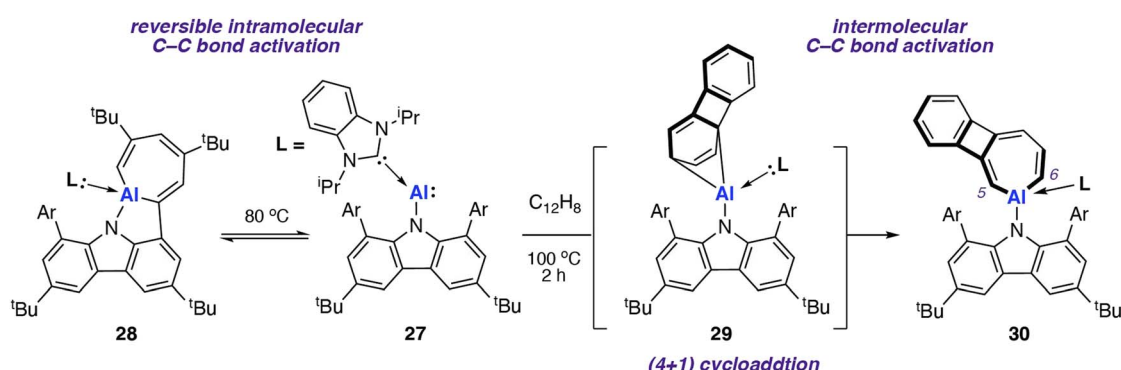
Scheme 9 Intra- (left) and inter-(right) C–C bond activation with NHC coordinated aluminylene **27**. Ar = 3,5-di-*tert*-butylphenyl.
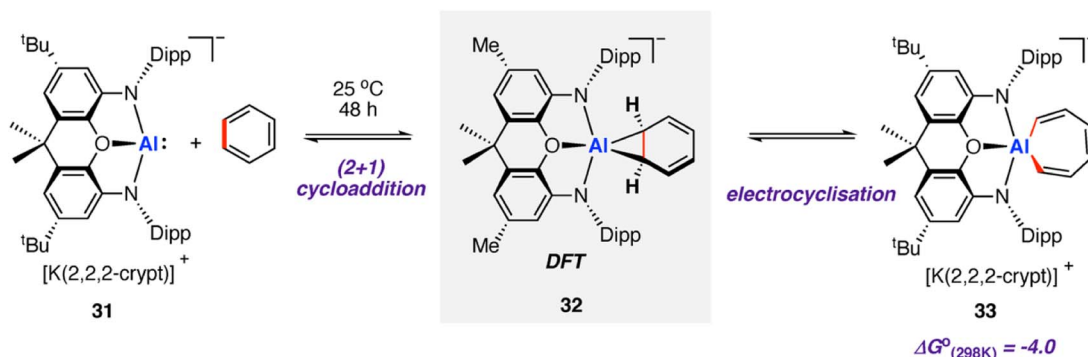
Scheme 10 Reversible insertion of aluminium(I) complex **31** into the C–C bond of benzene.
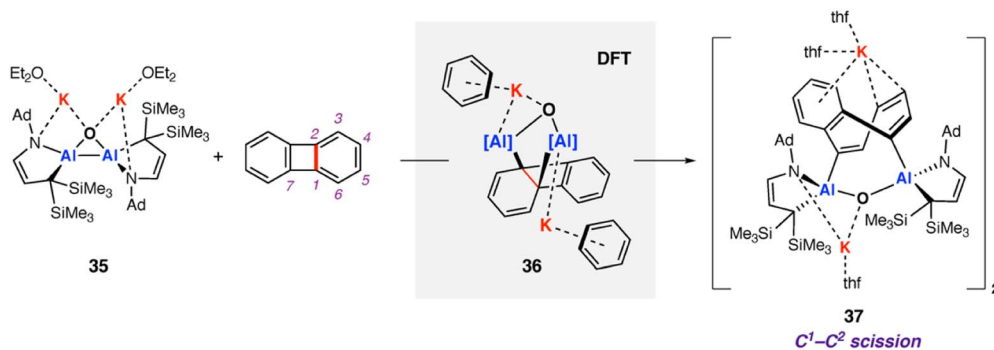
Scheme 11 Reaction of dianionic dialane complex **35** with biphenylene. C^1–C^2 activation of biphenylene observed in the product **37**. Note: line-drawing for **37** has been represented as in the original publication.

in moderate (31%) yield. Multinuclear NMR spectroscopy and X-ray diffraction analysis showed the dimeric product **37**, formed by unusual C–C bond cleavage of the C^1–C^2 bond in biphenylene. DFT calculations were employed to gain insight into a likely reaction mechanism. Coordination of biphenylene to potassium antedates Al–Al bond cleavage and Al–C bond formation. The initial reaction step involves coordination of **35** to form the biphenylene adduct. Two subsequent 1,3-sigmatropic rearrangements result in migration of the Al centre across the hydrocarbon scaffold to form **36** ($\Delta G^{\ddagger}_{298\ K} = 19.9$ then 25.8 kcal mol^{-1}). **36** contains a five-membered AlOC$_2$Al ring, primed for C–C bond activation. C–C bond activation proceeds via a low energy transition state ($\Delta G^{\ddagger}_{298\ K} = 3.4$ kcal mol^{-1}) to give the observed product **37**. The overall process from **35** and biphenylene to **37** is exergonic ($\Delta G^{\circ}_{298\ K} = -12.0$ kcal mol^{-1}). The K$^+$ ions were modelled explicitly in this pathway and may play an important role in structural organization and facilitating C–C bond activation.

In 2022, Braunschweig and co-workers reported an in situ generated base-stabilised aryl aluminene (viz. aluminylene) complex capable of deconstructing benzene and toluene via

C–C bond scission (Scheme 12).[78] The reaction was very low yielding toward the C–C activation product (3–5% isolated yield) with the major product formed via an intramolecular C–H activation of the mesityl ligand. Reduction of the parent NHC-coordinated aluminium diiodo complex [Al(NHC)Ar*(I)$_2$] (NHC = 1,3,4,5-tetramethylimidazol-2-ylidene; Ar* = 2,6-C$_6$H$_3$Mes$_2$, Mes = 2,4,6-trimethylphenyl) **38** with KC$_8$ yielded a mixture of C–H and C–C **41a–b** activation products. The reaction mechanism was proposed to proceed via formation of di-aluminene complex [{Al(NHC)Ar*}$_2$] **39** and subsequent monomerisation to the reactive aluminium(I) nucleophile [Al(NHC)Ar*] **40**. As these species are generated in situ, however, the speciation of the aluminium complexes and role of K$^+$ remains ambiguous.

Coordination of the NHC ligand was essential to increase the reactivity of the aluminium centre, facilitating the observed C–C bond activation. A related base free aluminene was reported previously and showed no reactivity toward aromatic solvents.[79] DFT calculations suggest that the frontier molecular orbitals of **40** are aluminium-based. Coordination of the NHC ligand decreases the HOMO–LUMO gap from 3.82 eV to 3.23 eV, with
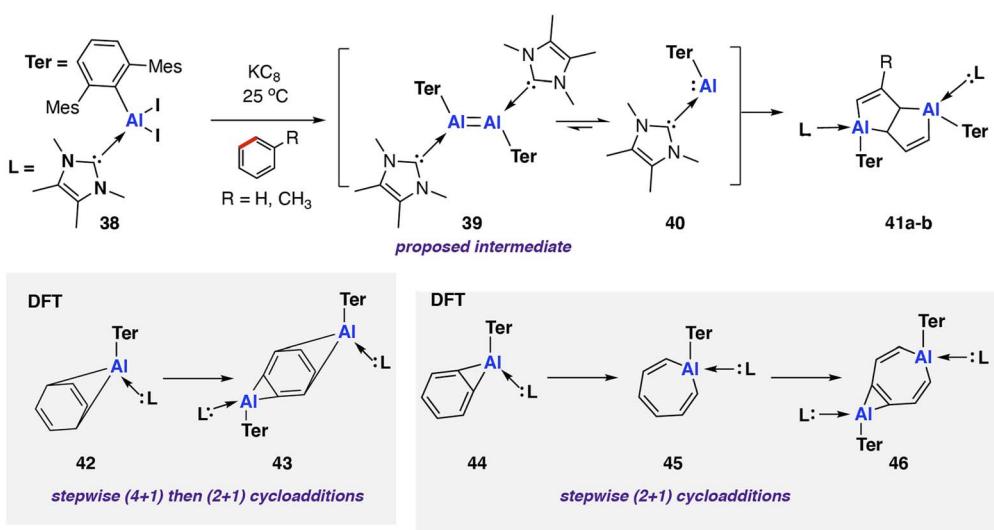
Scheme 12 C–C bond scission of benzene and toluene by an in situ generated NHC-coordinated aluminylene **41** (Mes = 2,4,6-trimethylphenyl; **42a** R = H; **42b** R = CH$_3$).

an increase in the HOMO energy the major contribution to the change.

Further calculations were performed to investigate a likely reaction mechanism to form pentalene complex **41a**; for computational cost, a truncated analog of **40** was used $[\text{Al(NHC')Ar'}]$ (NHC' = 1,5-dimethylimidazol-2-ylidene; Ar' = $2,6\text{-}C_6H_3Xyl_2$, Xyl = 2,6-dimethylphenyl). Two potential mechanisms were investigated computationally. The authors comment that both pathways are feasible with low and reversible energy barriers for C–C bond activation and are likely competing. The first pathway, analogous to the reaction of **20** with biphenylene,[75] proceeds *via* a $(4 + 1)$ cycloaddition by the aluminylene with benzene, followed by a $(2 + 1)$ cycloaddition from another equivalent of **40** on the opposite face of the benzene molecule to create a bimetallic complex **43**. Rearrangement and concomitant C–C bond activation of the benzene unit yields **41a** in an overall exergonic process ($\Delta G^{\ddagger}_{298\ K} = 25.8$ kcal mol^{-1}; $\Delta G^{\circ}_{298\ K} = -38.1$ kcal mol^{-1}).

The second pathway involves an initial formal insertion of aluminylene **40** into the C–C bond of benzene *via* an initial $(2 + 1)$ cycloaddition forming an aluminocyclopropane intermediate **44**. Reaction of a second equivalent of **40** with this intermediate again facilitates C–C bond cleavage, yielding the observed product **41a** ($\Delta G^{\ddagger}_{298\ K} = 17.4$ kcal mol^{-1}).

3. Conclusions and perspective

Carbon–carbon bond activation facilitated by main-group and post-transition metal complexes is gathering increasing attention. The above summary of known examples of this type of reactivity shows that main-group metal complexes can mimic, and complement, reactivity long associated with late transition metals. Common to several of these systems is the idea that the key factor is the ability to install the electropositive and coordinatively unsaturated metal atom *e.g.* Mg, Al, or Zn, in a suitable position on a hydrocarbon framework to facilitate migration/rearrangement reactions. Surprisingly redox based processes, *e.g.* oxidative addition, are not often invoked in the actual C–C bond breaking step, this contrasts examples with transition metals where they are common. The divergence in behaviour may well reflect the spatial availability of the orbitals involved in reactivity, with main group and post-transition metal complexes typically characterised by spatially orthogonal HOMO and LUMO orbitals with large energy separation, while transition metals often have a manifold of multiple available d-orbitals, which (in combination) are more spatially flexible.

In this regard, it is notable that many of the emerging applications of low-valent aluminium in C–C bond activation rely on low-oxidation state complexes with coordinated ligands (*e.g.* NHCs). The coordination event not only lowers the HOMO–LUMO gap it also changes the geometry at the metal centre. Both may be important in reaching accessible transition states for C–C bond activation that might not otherwise be possible with the ligand-free counterparts. Similarly, cooperative effects between two or more metals offer alternative pathways to break C–C bonds with reagents that are constrained to a certain set of orbital interactions. Bimetallic pathways have been invoked in several of the systems known to date., with two metals acting in concert; binding, distorting, and destabilising hydrocarbon frameworks to achieve C–C bond activation.

In the immediate future, it is likely that new and interesting examples of C–C bond activation with main group and post-transition metals will be discovered. Investigation of low-valent aluminium reagents appears to be a particularly fertile area. Systematic studies that aim to generate an understanding of why examples of C–C bond activation with certain metals are so prevalent, and what factors influence reactivity (*e.g.* coordination geometry, orbital energies, orbital symmetry, electronegativity of M, M–C bond dissociation energies) will help the field develop. Only a small number of main group and post-transition metal elements have been reported to facilitate C–C bond activation. Investigation of complexes of electrophilic main group metals such as those of Ca, Sr, Ba, Ga, In, Sn, and Pb is warranted and may bring with it new mechanistic insight and/or opportunities to control selectivity by tuning the metal site. The scope of reactivity described so far spans some of the most activated strained cycloalkanes and least reactive aromatic carbon rings. There is enormous opportunity in the middle ground. Expansion of examples of C–C bond activation to medium and large cycloalkane rings along with fragmentation of branched and linear alkane chains are obvious targets for the field.

Catalytic protocols for C–C bond functionalisation *e.g.* through hydrosilylation are beginning to emerge. There is a clear need for development of new catalysts for C–C bond functionalisation. The ability to alter hydrocarbon scaffolds of complex organic molecules and to valourise simple hydrocarbons or aromatics through catalysis are particularly attractive approaches that have long been associated with late transition metals. In the longer term, such catalytic transformations could underpin sustainable chemical manufacturing practices including the valourisation of molecules from biomass or the recycling of hydrocarbon-based polymers. The efforts described above suggest that main group systems have the potential to make important contributions in these areas that complement transition metal systems while also addressing key aspects of element scarcity, supply chain risk, and sustainability.

Author contributions

Both authors contributed to the writing of this manuscript.

Conflicts of interest

There are no conflicts to declare.

Acknowledgements

Notes and references

1 B. Wang, M. A. Perea and R. Sarpong, *Angew. Chem., Int. Ed.*, 2020, **59**, 18898–18919.

2 M. Murakami and N. Ishida, *J. Am. Chem. Soc.*, 2016, **138**, 13759–13769.

3 R. Watanabe, T. Suzuki and T. Okuhara, *Catal. Today*, 2001, **66**, 123–130.

4 D. S. J. Jones and P. R. Pujado, *Handbook of Petroleum Processing*, Springer, 2006, pp. 1–841.

5 G. B. Mcvicker, M. Daage, M. S. Touvelle, C. W. Hudson, D. P. Klein, W. C. Baird, B. R. Cook, J. G. Chen, S. Hantzer, D. E. W. Vaughan, E. S. Ellis and O. C. Feeley, *J. Catal.*, 2002, **210**, 137–148.

6 S. Hu, T. Shima and Z. Hou, *Nature*, 2014, **512**, 413–415.

7 S. J. Blanksby and G. B. Ellison, *Acc. Chem. Res.*, 2003, **36**, 255–263.

8 X. Qiu, Y. Sang, H. Wu, X. S. Xue, Z. Yan, Y. Wang, Z. Cheng, X. Wang, H. Tan, S. Song, G. Zhang, X. Zhang, K. N. Houk and N. Jiao, *Nature*, 2021, **597**, 64–69.

9 K. Ruhland, *Eur. J. Org. Chem.*, 2012, **14**, 2683–2706.

10 V. M. Benitez, J. M. Grau, J. C. Yori, C. L. Pieck and C. R. Vera, *Energy Fuels*, 2006, **20**, 1791–1798.

11 F. P. Guengerich and F. K. Yoshimoto, *Chem. Rev.*, 2018, **118**, 6573–6655.

12 T. D. H. Bugg and C. J. Winfield, *Nat. Prod. Rep.*, 1998, **15**, 513–530.

13 M. Gozin, A. Welsman, Y. Ben-David and D. Milstein, *Nature*, 1993, **364**, 699–701.

14 C. Jun, *Chem. Soc. Rev.*, 2004, **33**, 610–618.

15 M. Murakami and T. Matsuda, *Chem. Commun.*, 2011, **47**, 1100–1105.

16 C. T. To and K. S. Chan, *Eur. J. Org. Chem.*, 2019, **2019**, 6581–6591.

17 L. Souillart and N. Cramer, *Chem. Rev.*, 2015, **115**, 9410–9464.

18 M. E. Van Der Boom, H. Kraatz, Y. Ben-david and D. Milstein, *Chem. Commun.*, 1996, **18**, 2167–2168.

19 K. C. Bishop, *Chem. Rev.*, 1976, **76**, 461–486.

20 K. B. Wiberg, *Angew. Chem., Int. Ed.*, 1986, **25**, 312–322.

21 T. Dudev and C. Lim, *J. Am. Chem. Soc.*, 1998, **120**, 4450–4458.

22 R. D. Bach and O. Dmitrenko, *J. Am. Chem. Soc.*, 2004, **126**, 4444–4452.

23 M. E. O'Reilly, S. Dutta and A. S. Veige, *Chem. Rev.*, 2016, **116**, 8105–8145.

24 β-Alkyl migration can be defined as a subclass of β-alkyl elimination, wherein the substrate remains intact on the metal centre throughout the reaction.

25 H. Fruhauf, *Chem. Rev.*, 1997, **97**, 523–596.

26 S. Reymond and J. Cossy, *Chem. Rev.*, 2008, **108**, 5359–5406.

27 E. Lèbre, M. Stringer, K. Svobodova, J. R. Owen, D. Kemp, C. Côte, A. Arratia-Solar and R. K. Valenta, *Nat. Commun.*, 2020, **11**, 1–8.

28 C. Church and A. Crawford, *The Geopolitics of the Global Energy Transition*, 2020, 73, pp. 279–304.

29 P. P. Power, *Nature*, 2010, **463**, 171–177.

30 J. G. M. Morton, M. A. Dureen and D. W. Stephan, *Chem. Commun.*, 2010, **46**, 8947–8949.

31 Z. Y. Zhang, Z. Y. Liu, R. T. Guo, Y. Q. Zhao, X. Li and X. C. Wang, *Angew. Chem., Int. Ed.*, 2017, **56**, 4028–4032.

32 Z. Y. Zhang, J. Ren, M. Zhang, X. F. Xu and X. C. Wang, *Chin. J. Chem.*, 2021, **39**, 1641–1645.

33 H. Suzuki, N. Tokitoh and R. Okazaki, *J. Am. Chem. Soc.*, 1994, **116**, 11572–11573.

34 D. Wendel, A. Porzelt, F. A. D. Herz, D. Sarkar, C. Jandl, S. Inoue and B. Rieger, *J. Am. Chem. Soc.*, 2017, **139**, 8134–8137.

35 A. Roy, V. Bonetti, G. Wang, Q. Wu, H. F. T. Klare and M. Oestreich, *Org. Lett.*, 2020, **22**, 1213–1216.

36 L. L. Liu, J. Zhou, L. L. Cao, R. Andrews, R. L. Falconer, C. A. Russell and D. W. Stephan, *J. Am. Chem. Soc.*, 2018, **140**, 147–150.

37 K. Liu, G. Wang, Z. W. Zhang, Y. Y. Shi and Z. S. Ye, *Org. Lett.*, 2022, **24**, 6489–6493.

38 J. Ren, F. H. Du, M. C. Jia, Z. N. Hu, Z. Chen and C. Zhang, *Angew. Chem., Int. Ed.*, 2021, **60**, 24171–24178.

39 During the revision of this manuscript, a review article covering a similar area was published: S. Fujimori, A. Kostenko and S. Inoue, *Chem.–Eur. J.*, 2023, e202301973.

40 W. Pfohl, *Liebigs Ann.*, 1960, **629**, 207–209.

41 D. Dakternieks, A. E. K. Lim and K. F. Lim, *Chem. Commun.*, 1999, **15**, 1425–1426.

42 R. Y. Kong and M. R. Crimmin, *J. Am. Chem. Soc.*, 2020, **142**, 11967–11971.

43 C. Jones, *Nat. Rev.*, 2017, **1**, 1–9.

44 S. P. Green, C. Jones and A. Stasch, *Science*, 2007, **318**, 1754–1758.

45 S. J. Bonyhady, C. Jones, S. Nembenna, A. Stasch, A. J. Edwards and G. J. Mcintyre, *Chem.–Eur. J.*, 2010, **16**, 938–955.

46 A. Stasch and C. Jones, *Dalton Trans.*, 2011, **40**, 5659–5672.

47 A. J. Boutland, A. Carroll, C. Alvarez Lamsfus, A. Stasch, L. Maron and C. Jones, *J. Am. Chem. Soc.*, 2017, **139**, 18190–18193.

48 S. P. Green, C. Jones and A. Stasch, *Angew. Chem., Int. Ed.*, 2008, **47**, 9079–9083.

49 J. M. Parr, A. Phanopoulos, A. Vickneswaran and M. R. Crimmin, *Chem. Sci.*, 2023, **14**, 1590–1597.

50 C. P. Casey, S. L. Hallenbeck, D. W. Pollock and C. R. Landis, *J. Am. Chem. Soc.*, 1995, **117**, 9770–9771.

51 D. Dange, A. R. Gair, D. D. L. Jones, M. Juckel, S. Aldridge and C. Jones, *Chem. Sci.*, 2019, **10**, 3208–3216.

52 L. Garcia, C. Dinoi, M. F. Mahon, L. Maron and M. S. Hill, *Chem. Sci.*, 2019, **10**, 8108–8118.

53 J. Spielmann, D. Piesik, B. Wittkamp, G. Jansen and S. Harder, *Chem. Commun.*, 2009, **23**, 3455–3456.

54 D. Svatunek and K. N. Houk, *J. Comput. Chem.*, 2019, **40**, 2509–2515.

55 P. Vermeeren, S. C. C. van der Lubbe, C. Fonseca Guerra, F. M. Bickelhaupt and T. A. Hamlin, *Nat. Protoc.*, 2020, **15**, 649–667.

56 C. Bakewell, *Dalton Trans.*, 2020, **49**, 11354–11360.

57 M. Rauch, S. Ruccolo and G. Parkin, *J. Am. Chem. Soc.*, 2017, **139**, 13264–13267.

58 W. D. Jones, in *C–C Bond Activation*, ed. G. Dong, Springer Berlin Heidelberg, Berlin, Heidelberg, 2013, pp. 1–31.

59 M. Zhu, Z. Chai, Z. Lv, T. Li, W. Liu, J. Wei and W. Zhang, *J. Am. Chem. Soc.*, 2023, **145**, 6633–6638.

60 A. Velian, S. Lin, A. J. M. Miller, M. W. Day and T. Agapie, *J. Am. Chem. Soc.*, 2010, **132**, 6296–6297.

61 H. Takano, T. Ito, S. Kanyiva and T. Shibata, *Eur. J. Org. Chem.*, 2019, **18**, 2871–2883.

62 A. B. Chaplin, R. Tonner and A. S. Weller, *Organometallics*, 2010, **29**, 2710–2714.

63 C. Perthuisot, B. L. Edelbach, D. L. Zubris and W. D. Jones, *Organometallics*, 1997, **16**, 2016–2023.

64 C. Perthuisot and W. D. Jones, *J. Am. Chem. Soc.*, 1994, **116**, 3647–3648.

65 J. J. Elsch, A. M. Plotrowski, I. Kyoung, C. Kruger and Y. H. Tsay, *Organometallics*, 1985, **4**, 224–231.

66 K. Koshino and R. Kinjo, *J. Am. Chem. Soc.*, 2020, **142**, 9057–9062.

67 F. Xu and J. Zhu, *Chem.–Eur. J.*, 2023, **29**, e202203216.

68 J. Hicks, P. Vasko, J. M. Goicoechea and S. Aldridge, *J. Am. Chem. Soc.*, 2019, **141**, 11000–11003.

69 J. J. Cabrera-Trujillo and I. Fernández, *Chem.–Eur. J.*, 2020, **26**, 11806–11813.

70 J. M. Parr, A. J. P. White and M. R. Crimmin, *Chem. Sci.*, 2022, **13**, 6592–6598.

71 C. Cui, S. Köpke, R. Herbst-Irmer, H. W. Roesky, M. Noltemeyer, H. G. Schmidt and B. Wrackmeyer, *J. Am. Chem. Soc.*, 2001, **123**, 9091–9098.

72 X. Zhang and L. L. Liu, *Angew. Chem., Int. Ed.*, 2022, **61**, e2021166.

73 X. Zhang and L. L. Liu, *Angew. Chem., Int. Ed.*, 2021, **60**, 27062–27069.

74 A. Hinz and M. P. Müller, *Chem. Commun.*, 2021, **57**, 12532–12535.

75 R. Y. Kong and M. R. Crimmin, *Angew. Chem., Int. Ed.*, 2021, **60**, 2619–2623.

76 C. Bakewell, M. Garçon, R. Y. Kong, L. O'Hare, A. J. P. White and M. R. Crimmin, *Inorg. Chem.*, 2020, **59**, 4608–4616.

77 K. Koshino and R. Kinjo, *J. Am. Chem. Soc.*, 2021, **143**, 18172–18180.

78 D. Dhara, A. Jayaraman, M. Härterich, R. D. Dewhurst and H. Braunschweig, *Chem. Sci.*, 2022, **13**, 5631–5638.

79 J. D. Queen, A. Lehmann, J. C. Fettinger, H. M. Tuononen and P. P. Power, *J. Am. Chem. Soc.*, 2020, **142**, 20554–20559.